Computation of simultaneous available transfer capability under voltage and thermal security constraints

Florin Capitanescu
University of Liège
Belgium
capitane@montefiore.ulg.ac.be

Thierry Van Cutsem
FNRS (National Fund for Scientific Research)
University of Liège, Belgium
t.vancutsem@ulg.ac.be

Abstract - **This paper proposes a method to compute the Available Transfer Capability (ATC) of a power system under both thermal and voltage security constraints. The objective is to determine, in some optimal manner, the ATC of several simultaneous transactions, such that any postulated contingency does not cause voltage instability nor thermal overloads. Thermal constraints are derived for every branch likely to be overloaded in post-contingency states. Voltage security constraints are derived from voltage unstable post-contingency scenario, obtained by Quasi Steady-State simulation, a fast time-domain method. The paper also addresses the discrimination problem, i.e. the fact that the computed ATC might favor some trades to the detriment of others. Variants will be discussed to deal with such situations. The method is illustrated on an 80-bus test system.**

Keywords: **Available transfer capability, voltage security, thermal overload, dynamic security analysis**.

1 INTRODUCTION

Electricity market deregulation now prevails in many countries. In a deregulated environment a crucial information is the determination of the ATCs relative to all foreseen trade paths [1]. The ATC values may be posted on a Website so that each market player can use them in order to make reservation. Each ATC represents the maximal increment of power which can be transmitted from a source to a sink without violating any security constraint. The latter may involve static (circuit loading, voltage profile, etc.), voltage stability and angle stability constraints. This paper deals with thermal overload and voltage stability constraints.

Most methods for computing ATC proposed up to now focus on thermal constraints [2, 3, 4, 5]. They are based on the very fast DC load flow model. Although valid in many practical cases, the DC approximation may be less satisfactory when voltage and thermal aspects are strongly coupled, in which case the full AC load flow model would be more appropriate. However, much less has been done for voltage stability constraints. Ref. [6] used the continuation power flow method. To deal with dynamic aspects while retaining the computational efficiency of load flow type methods, Refs. [7, 8] used Quasi Steady-State (QSS) simulation, a fast time-domain method.

A drawback of these approaches is that ATCs are computed separately for each transaction. Clearly, when several transactions take place simultaneously modifying the volume of one trade will affect to some extent the ATC of all the other trades. This interdependence makes it necessary to consider several transactions simultaneously in the ATC computation.

A first approach to this new problem was presented in [5]. It consists in maximizing, in the L_1 sense, the sum of all possible transactions under linearized operating constraints corresponding to circuit loading, bus voltage magnitude and generator reactive power. More recently, Ref. [9] proposed to maximize the product of transactions over a security region bounded by linearized operating constraints based on load flow equations.

In this paper we propose a method to compute simultaneous ATCs under both thermal and voltage security constraints. The latter involve contingencies. The ATC value is the result of an optimization problem in which we maximize the use of the network by the various involved traders. Thermal constraints are derived for every branch likely to be overloaded in post-contingency states. Voltage security constraints are derived from voltage unstable post-contingency scenarios analyzed by QSS simulation.

2 STATEMENT OF THE PROBLEM

2.1 Transaction definition

A transaction is a bilateral exchange of power between a selling and a buying entity. In the sequel, the selling (resp. buying) entity is called source (resp. sink) and may comprise several generators (resp. loads). The k-th transaction ($k = 1, \ldots, t$) is defined by its volume T_k, which is the active power received by the sink, as well as by the bus participations in the source and the sink. The latter are defined by the two m-dimensional vectors:

$$\boldsymbol{\alpha}_k = [\alpha_{k1} \ldots \alpha_{ki} \ldots \alpha_{km}]^T \quad \boldsymbol{\beta}_k = [\beta_{k1} \ldots \beta_{ki} \ldots \beta_{km}]^T$$

where m is the total number of buses and α_{ki} (resp. β_{ki}) is the participation factor of the generator (resp. load) at bus i in the k-th transaction. Obviously, $\alpha_{ki} = 0$ (resp. $\beta_{ki} = 0$) in the absence of a participating generator (resp. load) at bus i, and $\alpha_{ki} > 0$ (resp. $\beta_{ki} > 0$) otherwise. Furthermore, the participation factors are chosen such that:

$$\sum_{i=1}^{m} \alpha_{ki} = 1 + \delta_k \quad \sum_{i=1}^{m} \beta_{ki} = 1$$

where δ_k accounts for the transmission losses associated with the k-th transaction.

Thus, for the k-th transaction, the active power P_i^+ *injected into* ($i = 1, \ldots, m$) and the active power P_i^- *drawn from* the i-th bus relate to the above variables through:

$$P_{ki}^+ = \alpha_{ki} T_k \quad P_{ki}^- = \beta_{ki} T_k \quad P_{ki}^+,\ P_{ki}^- \geq 0$$

and hence the volume of the k-th transaction is given by:

$$T_k = \sum_{i=1}^{m} P_{ki}^- = \frac{\sum_{i=1}^{m} P_{ki}^+}{1 + \delta_k} \quad \text{with} \quad 0 \leq T_k \leq T_k^{max}$$

where T_k^{max} is the minimum among the generation reserve and the maximal load consumption, for the corresponding participating generators and loads.

Denoting by Δ the variations from base case values, we have:

$$\Delta P_{ki}^+ = \alpha_{ki} \Delta T_k \qquad \Delta P_{ki}^- = \beta_{ki} \Delta T_k$$

and the net power variation at bus i is, for all transactions:

$$\Delta P_i = \sum_{k=1}^{t} \Delta P_{ki}^+ - \Delta P_{ki}^- = \sum_{k=1}^{t} (\alpha_{ki} - \beta_{ki})\, \Delta T_k \quad (1)$$

This equation defines a mapping between the space of power injections and the one of transactions.

2.2 Secure transaction region and simultaneous ATC

Let us consider the t-dimensional space of transactions. Each point of this space corresponds to a particular value of the pre-contingency transactions.

We define the *secure transaction region* $\mathcal{S}$ as the set of points of the transaction space such that no contingency of a specified list causes thermal overload nor voltage instability. ATCs are associated with points lying on the boundary $\mathcal{B}$ of this secure region $\mathcal{S}$.

The concept of simultaneous ATC is best illustrated on the following bi-dimensional example. Let us consider the space of two transactions T_1 and T_2 as depicted in Fig. 1. Lower and upper bounds restrict the transaction space to the interior of rectangle OGEF. Moreover, let us assume for simplicity that the secure transaction region $\mathcal{S}$ is further bounded by the line AB.

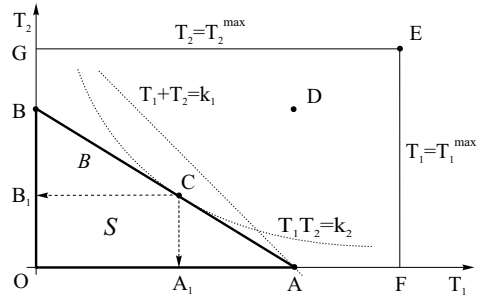

Figure 1: secure region and ATCs in a 2D-transaction space

If each transaction is considered separately, the ATC for T_1 (resp. T_2) corresponds to point A (resp. B). Now, if both transactions were accepted at these maximal values the system would operate at point D, outside the secure region. It is thus necessary to compute ATCs by maximizing a function of T_1 and T_2 while taking into account the boundary $\mathcal{B}$, which expresses the influence between the two transactions.

The first function to come to mind for the simultaneous ATC computation is the sum of transactions [5], namely:

$$\max_{T_1, T_2 \in \mathcal{S}} (T_1 + T_2)$$

This objective is directly related to the maximum use of the network. However, in our simple example, the solution of this optimization problem is point A, where transaction T_2 is zero ! In other words, maximizing the above L_1 norm tends to allocate network capacity to the transaction with the least effect on security. This may be considered discriminatory, especially when both transactions have almost equal effects, which corresponds in Fig. 1 to a boundary $\mathcal{B}$ almost parallel to the equi-$(T_1 + T_2)$ lines. In this case, a mere change in slope from -44 to -46 degrees, for instance, causes the optimum to jump from A to B !

Admittedly, this effect is less pronounced when the boundary is piece-wise linear (and convex) or when the box constraints are more limiting (point F lying in between O and A): T_2 is then nonzero at the optimum.

An alternative, however, is to maximize the product of transactions [9], namely:

$$\max_{T_1, T_2 \in \mathcal{S}} T_1 T_2$$

The optimum corresponds to point C, where an hyperbola $T_1 T_2 = k_2$ is tangent to the boundary $\mathcal{B}$. The ATC values correspond to the projections of point C on the axes (points A_1 and B_1). As can be seen, this objective is less discriminatory and, more importantly, allocates capacity to the transactions in proportion with their respective impact on security.

3 APPROXIMATION OF SECURITY BOUNDARY

3.1 Thermal overload constraints

When thermal overloads are of concern, the secure region $\mathcal{S}$ is the set of operating points such that no branch current is above its limit after a contingency, i.e.

$$I_j^{(r)} \leq I_j^{max} \qquad j = 1, \ldots, b \qquad r = 1, \ldots, c \qquad (2)$$

where b is the number of branches, c the number of specified contingencies, $I_j^{(r)}$ the current in the j-th branch after the r-th contingency and I_j^{max} the corresponding threshold value.

It is well known that (pre- or post-contingency) branch currents vary rather linearly with bus power injections. The inequality (2) can thus be linearized into:

$$I_{j,\,o}^{(r)} + \sum_{i=1}^{m} \frac{\partial I_j^{(r)}}{\partial P_i} \Delta P_i \leq I_j^{max} \qquad (3)$$

where $I_{j,\,o}^{(r)}$ is the post-contingency branch current for the base case value of the injections. The partial derivatives

are the sensitivities of the post-contingency branch currents to the pre-contingency injections. The latter can be determined using the DC load flow approximation [4] or from a well-known sensitivity formula involving the Jacobian of the steady-state equations (standard AC load flow or long-term equilibrium equations). Note that thermal overload constraints apply to the pre-contingency configuration as well but we assume for simplicity that post-contingency operating conditions are more severe.

Taking (1) into account, the inequality (3) can be rewritten in terms of transactions as:

$$I_{j,\,o}^{(r)} + \sum_{k=1}^{t}\sum_{i=1}^{m} \frac{\partial I_j^{(r)}}{\partial P_i}(\alpha_{ki} - \beta_{ki})\Delta T_k \leq I_j^{max} \qquad (4)$$

This formula yields the sensitivity of current $I_j^{(r)}$ to transaction T_k:

$$\frac{\partial I_j^{(r)}}{\partial T_k} = \sum_{i=1}^{m} \frac{\partial I_j^{(r)}}{\partial P_i}(\alpha_{ki} - \beta_{ki}) \qquad (5)$$

All such sensitivities can be computed in the base case.

The thermal security region $\mathcal{S}$ is thus bounded by linear constraints of type (4), and its boundary $\mathcal{B}$ is piecewise linear, each part corresponding to one of the constraints (4) active.

3.2 Voltage security constraints

When voltage instability is of concern, the security region $\mathcal{S}$ becomes the set of pre-contingency operating points such that the system responds in a stable way to any specified contingency.

We use QSS simulation to determine the system response to contingencies. This well-documented time-domain method [10] is fast while taking into account dynamic effects such as controls acting in the post-contingency configuration. Moreover, when coupled with small-disturbance analysis, this method can provide a linear approximation of the secure region boundary, as recalled hereafter.

The most common voltage instability mechanism is the loss of a long-term equilibrium [10] and hence we can approximate the secure region $\mathcal{S}$ as the set of pre-contingency operating points for which the system has a post-disturbance equilibrium. For a single contingency, a two-dimensional view of the power injection space is given in Fig. 2, where $\mathbf{P}_o$ corresponds to the base case and $\mathbf{P}_u$ to an unstable scenario.

Thus, if the contingency is applied to the system operating at point $\mathbf{P}_u$, instability results. The unstable system trajectory will "touch" the boundary $\mathcal{B}$ at a so-called *critical point* $\mathbf{P}_c$, identified through the change in sign of reactive generation to reactive load sensitivities [10].

Denoting the long-term equilibrium equations by:

$$\mathbf{g}(\mathbf{x}, \mathbf{P}) = \mathbf{g}(\mathbf{x}, \mathbf{P}_o + \Delta\mathbf{P}) = \mathbf{0} \qquad (6)$$

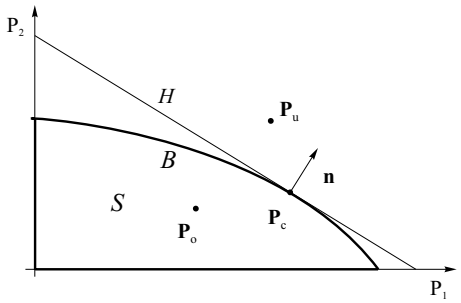

Figure 2: linear approximation of the voltage secure region

where $\mathbf{x}$ is the state vector, the normal vector $\mathbf{n}$ to the boundary $\mathcal{B}$ is given by [10]:

$$\mathbf{n} = \mathbf{g}_\mathbf{P}^T\,\mathbf{w} \qquad (7)$$

where $\mathbf{g_P}$ is the Jacobian of $\mathbf{g}$ with respect to $\mathbf{P}$ and $\mathbf{w}$ is the left eigenvector relative to the zero eigenvalue of the Jacobian $\mathbf{g_x}$ on the bifurcation surface $\mathcal{B}$.

From both $\mathbf{P}_c$ and $\mathbf{n}$, a linear approximation of the boundary surface $\mathcal{B}$ can be built, in the form of the tangent hyperplane $\mathcal{H}$ (see Fig. 2) whose equation is:

$$\mathbf{n}^\mathbf{T}(\mathbf{P} - \mathbf{P}_c) = 0 \qquad (8)$$

Let $\Delta\mathbf{P}$ be a vector of injection variations. In order $\mathbf{P}_o + \Delta\mathbf{P}$ to remain on the stable side of $\mathcal{H}$, $\Delta\mathbf{P}$ must satisfy:

$$\mathbf{n}^T(\mathbf{P}_o + \Delta\mathbf{P} - \mathbf{P}_c) \leq 0$$

or equivalently: $\displaystyle\sum_{i=1}^{m} n_i \Delta P_i \leq \mathbf{n}^T(\mathbf{P}_c - \mathbf{P}_o)$

Using (1), this inequality can be written in terms of transaction variations as:

$$\sum_{k=1}^{t} \tilde{n}_k \Delta T_k \leq C \qquad (9)$$

where $\displaystyle\tilde{n}_k = \sum_{i=1}^{m} n_i(\alpha_{ki} - \beta_{ki})$ and $C = \mathbf{n}^T(\mathbf{P}_c - \mathbf{P}_o)$

The voltage secure region is thus approximated by a set of linear inequalities, each corresponding to a contingency. For the r-th one $(r = 1, \ldots, u)$ we have:

$$\sum_{k=1}^{t} \tilde{n}_k^{(r)} \Delta T_k \leq C^{(r)} \qquad (10)$$

The piece-wise linear approximation of $\mathcal{B}$ is thus obtained by first setting the system to an operating point $\mathbf{P}_u$ where it responds to some contingencies in an unstable way, then extracting information from the corresponding unstable evolutions. Note that $\mathbf{P}_u$ does not appear explicitly in the so derived linear approximation (9); it is merely used to bring the system to instability. It does not appear either in the thermal overload constraints.

In practice, $\mathbf{P}_u$ is chosen so that all participating transactions are increased *beyond the expected ATC values* (so that this point falls outside the voltage secure region) and *equitably* (to avoid distortions). Such a choice admittedly requires some knowledge of the system under concern.

Incidentally, note that in congestion management, the problem of choosing $\mathbf{P}_u$ does not exist: this point is simply the operating point resulting from the various requested transactions. If it lies within the secure region, all the transactions can be accepted; otherwise, they must be curtailed in an optimal manner to bring $\mathbf{P}_u$ inside the secure region [11].

4 ATC COMPUTATION

4.1 Contingency filtering

In real-life applications, it is essential to quickly filter out harmless contingencies and limit the above analysis to the (potentially or effectively) dangerous ones.

As regards voltage instability, one can use a procedure similar to the one described in [8] within the context of single-transaction ATC calculations. The idea is that a contingency found stable at point $\mathbf{P}_u$ is harmless since this point is located outside the secure region defined by the most constraining contingencies. Furthermore, to save computing time, the various contingencies can be simulated at point $\mathbf{P}_u$ with a simple AC load flow and only those leading to divergence or causing voltage drops larger than some threshold are labelled potentially harmful. This threshold must be chosen small enough (conservative) to avoid missing dangerous contingencies but large enough to avoid too many false alarms. The potentially harmful contingencies are then analyzed in greater detail by QSS simulation, which filters out the false alarms. The remaining, harmful contingencies are kept for incorporation into the ATC calculation.

Note that in systems where long-term voltage stability is strongly influenced by post-contingency dynamic controls, a mere AC load flow might not be appropriate. QSS simulation must then be used to check all contingencies at point $\mathbf{P}_u$ [8]. Even in this case, the computation is much faster than with full time-domain simulation.

As regards thermal overloads, each post-contingency operating point provided by the AC load flow calculation (at the first filtering step) or by a stable QSS simulation (at the second step) is checked with respect to branch overloads. The corresponding contingencies are also kept for inclusion in the ATC calculation presented hereafter.

4.2 Linear ATC calculation

Under the linear approximations explained in the previous section, the ATC for the t simultaneous transactions can be obtained as the solution of the following optimization problem:

$$\max L_1 = \sum_{k=1}^{t} \Delta T_k \tag{11}$$

$$\text{or} \quad \max L_\pi = \prod_{k=1}^{t} \Delta T_k \tag{12}$$

subject to :

$$\sum_{k=1}^{t} \tilde{n}_k^{(r)} \Delta T_k \leq C^{(r)} \quad r = 1, \ldots, u \tag{13}$$

$$\sum_{k=1}^{t} \frac{\partial I_j^{(r)}}{\partial T_k} \Delta T_k \leq I_j^{max} - I_{j,o}^{(r)} \quad \begin{matrix} r = 1, \ldots, \ell \\ j = 1, \ldots, b(r) \end{matrix} \tag{14}$$

$$0 \leq \Delta T_k \leq T_k^{max} \tag{15}$$

where u is the number of voltage harmful contingencies identified in the filtering step, ℓ is the corresponding number of thermal harmful contingencies and $b(r)$ is the number of branches overloaded by the r-th contingency.

The L_1 objective (11) leads to a simple linear programming problem. The product objective (12), whose motivation has been explained in Section 2.2, leads to a geometric programming problem, for which we successfully used a successive quadratic programming solver.

One cannot exclude the case where a contingency would create both voltage and thermal problems. Now, if the point $\mathbf{P}_u$ has been taken outside the voltage secure region, the contingency is labelled voltage harmful in the filtering phase but, as the system does not reach an operating point where branch overloads can be checked, the latter problem is hidden. Two procedures can be thought of to face such situations:

- at the solution of the above optimization problem, check all voltage harmful contingencies for possible branch overloads. If some are detected, add the corresponding constraints (14) to the original set and perform a new optimization
- solve the voltage optimization problem (11 or 12, 13, 15) first. When all contingencies are stabilized, check thermal overloads, add the corresponding constraints (14) and perform a new optimization.

4.3 Heuristic handling of nonlinearities

The real boundary $\mathcal{B}$ is nonlinear and not necessarily smooth as assumed above. This is especially true for the voltage secure region. The constraints (13, 14) are only linear approximations of this complex boundary. In particular, the linearized optimization problem may yield a solution ΔT_k^* located (hopefully slightly) outside the secure region, or conservatively inside.

To improve the ATC computation while keeping it simple, the following heuristic procedure is used. First, we consider that the *relative* values of the various $\tilde{n}_k^{(r)}$ coefficients in (13) (i.e. the slope of the tangent hyperplane $\mathcal{H}$) are correct, but the location of the critical point $\mathbf{P}_c$ may be affected by some error. $\mathcal{H}$ is thus moved parallel to itself, expanding or contracting the linear approximation of the secure region. Thus, we replace (13) by:

$$f \sum_{k=1}^{t} \tilde{n}_k^{(r)} \Delta T_k \leq C^{(r)} \tag{16}$$

and adjust f iteratively to obtain the best objective function together with secure transactions ΔT_k^*. The bisection method is used to this purpose; it consists of building a smaller and smaller interval $[f_r \; f_a]$, such that the solution ΔT_k^* of the linearized optimization problem (11 or 12, 14, 15, 16) is secure for $f = f_a$ and insecure for $f = f_r$.

This is checked through *nonlinear* QSS simulations of the u harmful contingencies. At each step, the interval is divided into two equal parts; if the midpoint leads to a secure (resp. insecure) optimum, it is taken as the new upper (resp. lower) bound. The procedure is repeated until $f_a - f_r$ becomes smaller than a tolerance ϵ and f is set to f_a. The search starts with $f_r = 0, f_a = 1$ (resp. $f_r = 1, f_a = 2$) if the very first linearized optimization yields a secure (resp. insecure) set of transactions.

Ideally the technique should be applied to each constraint (13); however, to keep the procedure simple, and because not all constraints are active at the optimum, a single value f is used to correct all of them.

Besides, the normal vector $\mathbf{n}$ involved in the $\tilde{n}_k^{(r)}$ coefficients can be updated each time the simulation of a harmful contingency is found unstable.

Although linearization works better for currents, it is possible to somewhat improve the values of the sensitivities in (14). Once the post-contingency current $I_j^{(r)}$ has been obtained by AC load flow or QSS simulation, all sensitivities $\partial I_j^{(r)}/\partial T_k$ $(k = 1, \ldots, t)$ are multiplied by:

$$\frac{I_j^{(r)} - I_{j,o}^{(r)}}{\sum_{k=1}^{t} \frac{\partial I_j^{(r)}}{\partial T_k} \Delta T_k^* - I_{j,o}^{(r)}} \tag{17}$$

where the numerator is the real change in branch current between the optimum and the base case, and the denominator is the corresponding linear prediction. A single update of the sensitivities is usually enough.

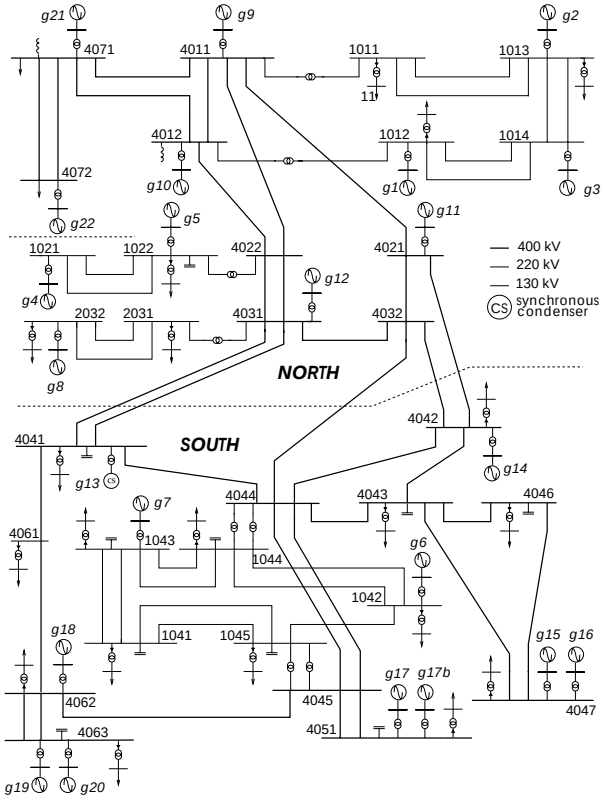

Figure 3: the (slightly modified) "Nordic 32" system

5 ILLUSTRATIVE EXAMPLE

We consider the 80-bus system shown in Figure 3, a variant of the "Nordic 32" system used e.g. by CIGRE Task Force 32.02.08 on Long-Term Dynamics (1995). A rather heavy power transfer takes place from the "North" to the "South" areas (see figure).

The QSS long-term simulation reproduces the dynamics of load tap changers and overexcitation limiters [7]. Generators respond to a disturbance according to governor control. The Southern generators having infinite speed droops, any power imbalance is covered by Northern generators, which may add to the North-South power flow.

We present examples of transmission capacity allocation to 10 simultaneous transactions. The source(s) and sink(s) as well as the upper bound of each transaction are given in Table 1.

Table 1: description of the involved transactions

transaction	source(s)	sink(s)	T_k^{max} (MW)
T_1	g21	4062	60
T_2	g22	4046	123
T_3	g4,g5	4051	99
T_4	g9,g10	1041,1045	115
T_5	g1,g2,g3	1011,1012,1013,1014	30
T_6	g8	2031	20
T_7	g19,g20	4047	17
T_8	g12	4043	30
T_9	g16	2032	40
T_{10}	g18	4042	70

A list of 49 contingencies is specified, which consist of single line or generator trippings.

$\mathbf{P}_u$ is taken as corresponding to a total transaction increase of 450 MW (with respect to the base case), equally shared by all transactions. The initial set of contingencies is simulated at this operating point. Ten contingencies lead to voltage instability (which confirms that $\mathbf{P}_u$ is outside the secure region) but no thermal overload is revealed. The linear constraints (13) are derived for each of the 10 contingencies.

Case A. The L_1 objective is maximized over the secure region. Thus the optimization problem (11, 13, 15) is solved, yielding an objective value of 239 MW. At this point, the system is stable with respect to all contingencies. Hence a larger ATC value is sought, using the technique of Section 4.3. The final value of the correction factor f is 0.4, and the objective increases to 279 MW.

The results are presented in the second column of Table 2. At the solution, most transactions are allowed to go up to their upper bound, except T_3 and T_4 (left at zero) and T_2 (for which no box constraint (15) is active).

Case B. The L_π objective (12) is now maximized over the secure region. Obviously, the harmful contingencies are the same and the system is voltage stability limited as in Case A.

The solution of the optimization procedure is shown in the third column of Table 2. As can be seen, this objective leads to allocate a nonzero power to all trades.

Table 2: simultaneous ATC results

transaction	case A	case B	case C	case D
T_1	60	18	0	6
T_2	12	17	0	5
T_3	0	16	0	5
T_4	0	17	0	5
T_5	30	30	30	30
T_6	20	20	20	20
T_7	17	17	17	17
T_8	30	30	24	7
T_9	40	40	40	40
T_{10}	70	70	70	24
$\sum_k T_k$	279	275	201	159

The solutions obtained with the two objectives differ by the first four transactions. In fact, the $\tilde{n}_k^{(r)}$ sensitivities of the latter are only slightly different (whatever the contingency) but the small differences are "amplified" by the L_1 objective, which favours the T_1 trade to the detriment of T_2, T_3 and T_4. The L_π objective, on the other hand, yields a more fair capacity allocation while keeping the total power transfer at almost the same value (only 4 MW less than with the L_1 objective). The allocation is in proportion with the impact on security.

Case C. In this case, and in the next one, the thermal limits of the 400-kV lines have been artificially decreased by 7 % to create thermal congestions.

Again, the L_1 objective is considered first. In this case, the system is thermal limited: the ATC is constrained by the loss of line 4011-4021 which causes the line 4031-4032 to be overloaded. This overload is partly due to a voltage drop at bus 4032 caused by the field current limitation of generator g11. In such a case, which could not be handled under the DC load flow approximation, the correction (17) proves useful. The solution of the optimization problem is shown in the fourth column of Table 2. The first four transactions are refused because the current in line 4031-4032 is most sensitive to these transactions. Transactions with the lowest sensitivities are accepted at their maximum.

Case D. The solution corresponding to the L_π objective is shown in the last column of Table 2. With respect to the previous case, transmission capacity is now allocated to the first four transactions, although to a little extent. Conversely, T_9, the only trade which can produce a counterflow in line 4031-4032, is accepted at its maximum. The same holds true for other trades which have less impact on that branch current.

A comparison of Cases C and D shows that significantly more (42 MW) network capacity is allocated with the L_1 objective. This is due to the fact that the current in branch 4031-4032 is almost equally sensitive to T_1, T_2, T_3, T_4 and T_8.

6 CONCLUSION

This paper has presented a method for computing the ATC of a power system under simultaneous transactions. The ATC is the solution of an optimization problem in which network usage is maximized under linear constraints which prevent any of the specified contingencies from causing thermal overload or voltage instability. Among the features of the proposed approach let us quote:
• a unified treatment of thermal and voltage security;
• the simultaneous handling of multiple contingencies;
• a heuristic technique to compensate for the linear approximation of the secure region. Further improvements of this technique are presently under investigation.

Two objective functions have been considered. While the L_1 objective maximizes the use of the transmission capacity, the L_π one yields a more fair allocation to the various transactions.

The method can be easily extended to:
• transmission capacity allocation through an implicit auction mechanism, by taking as objective function the sum of transactions, each weighted by its bid price;
• coordinated congestion management, in the case where all requested transactions cannot be accepted without endangering security.

REFERENCES

[1] P.W. Sauer, "Technical challenges of computing available transfer capability in electric power systems", 30th Annual Hawaii International Conference on System Sciences, Vol. V, January 1997, pp. 589-593

[2] M.H. Gravener and C. Nwankpa, "Available transfer capability and first order sensitivity", IEEE Trans. on Power Systems, Vol. 14, No. 2, May 1999, pp. 512-518

[3] G.A. Hamoud, "Assessment of available transfer capability of transmission systems", IEEE Trans. on Power Systems, Vol. 15, No. 1, February 2000, pp. 27-32

[4] R.D. Christie, B.F. Wollenberg and I. Wangensteen, "Transmission management in the deregulated environment", Proceedings of the IEEE, Vol. 88, No. 2, February 2000, pp. 170-195

[5] A.P.S. Meliopoulos and S.W. Kang, "An improved model for the evaluation of actual transfer capability in a deregulated environment", Bulk Power Systems Dynamics and control V, August 2001, Onomichi, Japan, pp. 203-209

[6] G.C. Ejebe, J. Tong, J.G. Waight, J.G. Frame, X. Wang and W.F. Tinney, "Available transfer capability calculations", IEEE Trans. on Power Systems, Vol. 13, No. 4, November 1998, pp. 1521-1527

[7] T. Van Cutsem, C. Moisse and R. Mailhot, "Determination of secure operating limits with respect to voltage collapse", IEEE Trans. on Power Systems, Vol. 14, February 1999, pp. 327-335

[8] T. Van Cutsem, F. Capitanescu, C. Moors, D. Lefebvre, V. Sermanson, "An advanced tool for preventive voltage security assessment", Proc. VIIth SEPOPE conference, Curitiba (Brazil), May 2000, paper IP-03

[9] C.Y. Li and C.W. Liu, "A new algorithm for available transfer capability computation", Electrical Power and Energy Systems, 2002, pp. 159-166

[10] T. Van Cutsem, C. Vournas, *Voltage stability of Electric Power Systems*, Kluwer Academic Publishers, Boston, 1998

[11] F.D. Galiana and M. Ilic, "A mathematical framework for the analysis and management of power transactions under power access", IEEE Trans. on Power Systems, Vol. 13, No. 2, May 1998, pp. 681-687